Electronic Supplementary Material (ESI) for Dalton Transactions.

Supplementary Information

Atomic Layer Deposition of $PbCl_2$, $PbBr_2$ and mixed lead halide (Cl, Br, I) PbX_nY_{2-n} thin films

Georgi Popov*[a], Goran Bačić[b], Charlotte Van Dijck[a], Laura S. Junkers[a], Alexander Weiß[a], Miika Mattinen[a], Anton Vihervaara[a], Mykhailo Chundak,[a] Pasi Jalkanen[c], Kenichiro Mizohata[c], Markku Leskelä[a], Jason D. Masuda[d], Seán T. Barry[b], Mikko Ritala*[a], Marianna Kemell[a]

[a.] *Department of Chemistry, University of Helsinki, P.O. Box 55, FI-00014 Helsinki, Finland*

[b.] *Department of Chemistry, Carleton University, 1125 Colonel By Drive, Ottawa, Ontario K1S 5B6, Canada*

[c.] *Department of Physics, University of Helsinki, P.O. Box 43, FI-00014 Helsinki, Finland*

[d.] *Department of Chemistry, Saint Mary's University, 923 Robie Street, Halifax, Nova Scotia B3H 3C3, Canada*

[*.] *Corresponding authors: georgi.popov@helsinki.fi, mikko.ritala@helsinki.fi*

CCDC 2180984 contains the supplementary crystallographic data for $(Pb(gem))_2$. These data can be obtained free of charge from the Cambridge Crystallographic Database Centre via https://www.ccdc.cam.ac.uk/structures/

Table of Contents

2.1 $Pb(btsa)_2$ and $SnCl_4$ process

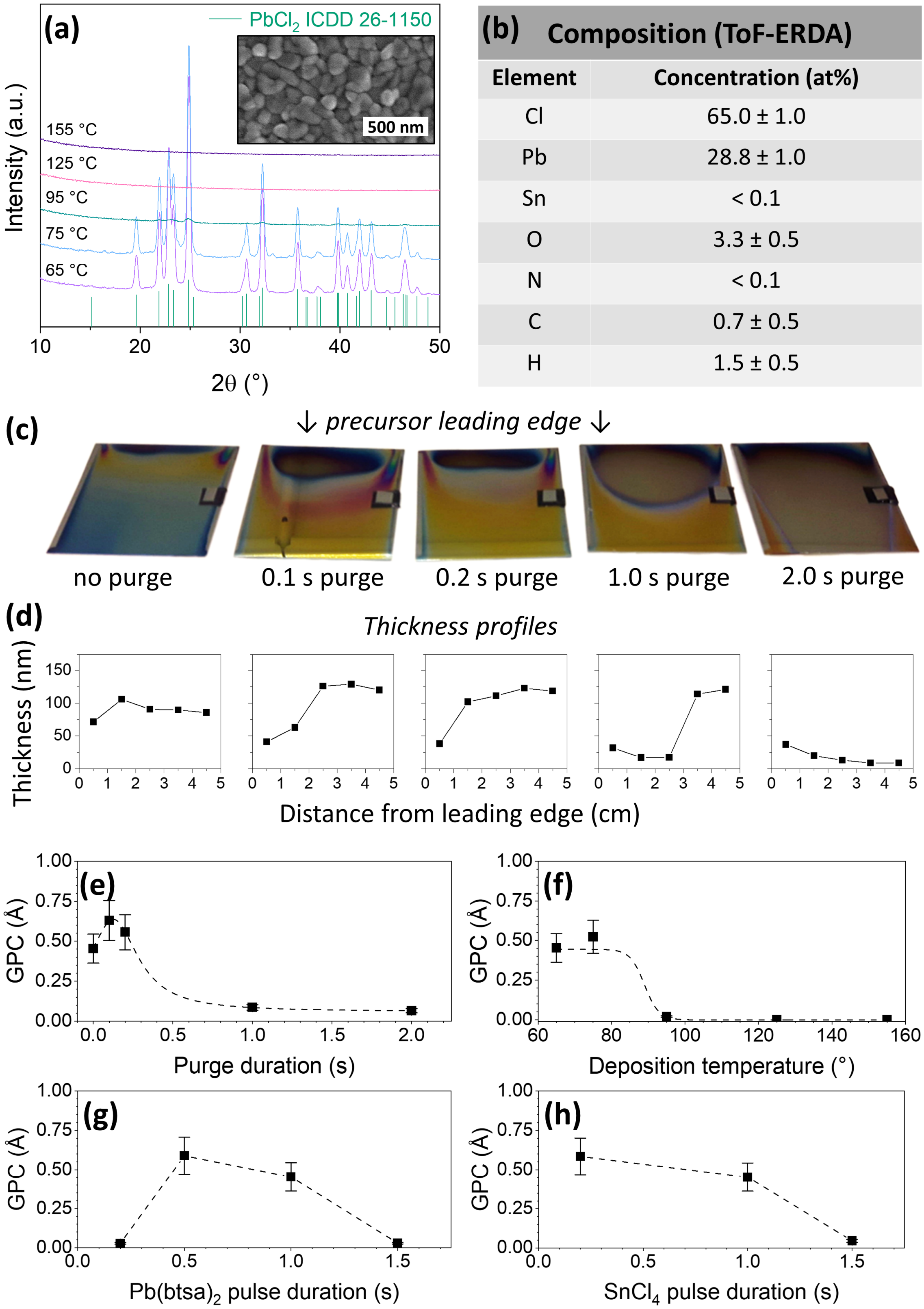

(b) Composition (ToF-ERDA)

Element	Concentration (at%)
Cl	65.0 ± 1.0
Pb	28.8 ± 1.0
Sn	< 0.1
O	3.3 ± 0.5
N	< 0.1
C	0.7 ± 0.5
H	1.5 ± 0.5

Figure S1. (a) XRD patterns of the $PbCl_2$ films deposited at different temperatures. Inset shows a FESEM image of a $PbCl_2$ film. (b) ToF-ERDA composition of a $PbCl_2$ film. (c) Digital photograph of $PbCl_2$ films deposited with different purge duration between the precursor pulses. Note that both purges were varied, i.e., 0.1 s purge means that both the purge after the $Pb(btsa)_2$ pulse and the purge after $SnCl_4$ pulse were 0.1 s long. (d) Thickness profiles of the films in (c). Growth per cycle (GPC) of $PbCl_2$ on silicon as a function (e) purge duration, (f) deposition temperature, (g) $Pb(btsa)_2$ pulse duration and (h) $SnCl_4$ pulse duration. In (e) the purge durations after both precursor pulses were varied. Unless otherwise evident, the data in this figure is from depositions made at 65 °C with 2000 cycles, 1 s long $Pb(btsa)_2$ and $SnCl_4$ pulse durations with no purge in between the pulses. Thicknesses were measured with EDS.

2.2 Pb(btsa)$_2$ and $TiCl_4$ process

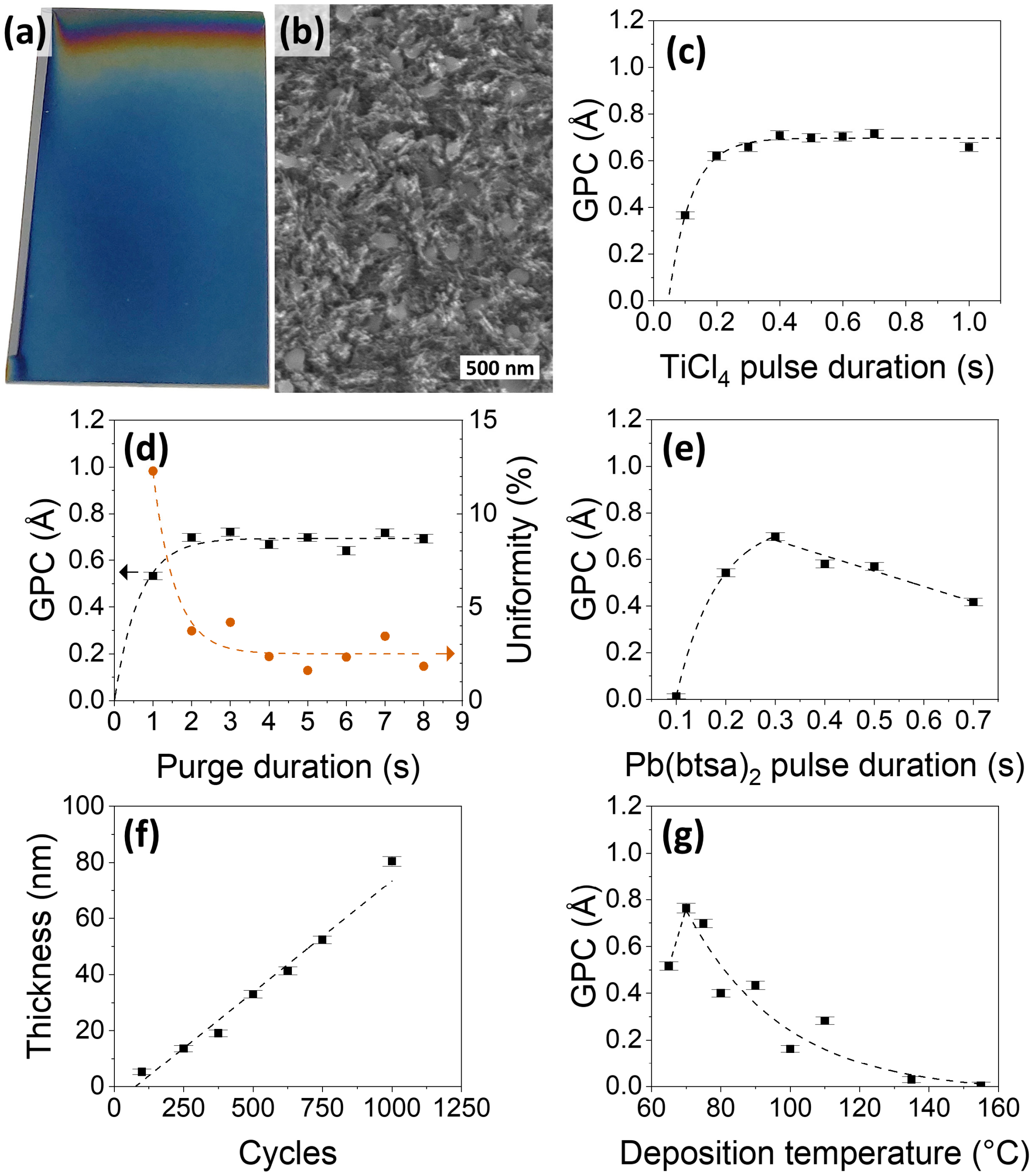

(h) Composition (ToF-ERDA)	
Element	**Concentration (at%)**
Cl	24.9 ± 1.5
Pb	24.0 ± 1.0
Ti	11.2 ± 1.0
O	30 ± 1.0
N	< 0.1
C	2.2 ± 0.5
H	6.9 ± 1.0

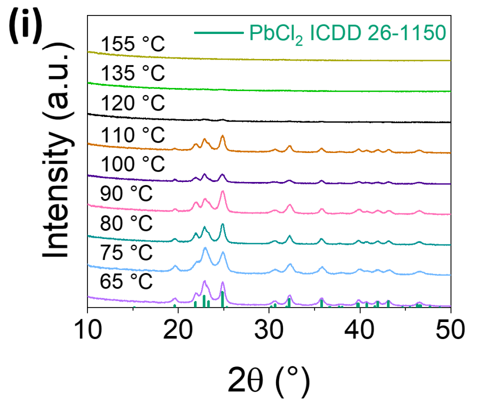

Figure S2. (a) Digital photograph and (b) FESEM image of a $PbCl_2$ film. GPC of $PbCl_2$ on silicon with a 2 nm Al_2O_3 underlayer as a function of (c) $TiCl_4$ pulse, (d) purge and (e) Pb(btsa)$_2$ pulse durations and (g) temperature. In (d) the purge durations after both precursor pulses were varied and film thickness uniformity is also shown. Uniformity was defined as standard deviation in thickness between 9 measurement points along precursor flow direction separated by 0.5 cm. (f) Thickness as a function of deposition cycles. (h) ToF-ERDA composition of a $PbCl_2$ film deposited on Si without an Al_2O_3 underlayer. (i) XRD patterns of the $PbCl_2$ films deposited at different temperatures. Unless otherwise evident, the data in this figure is from depositions made at 75 °C with 750 cycles, 0.3 s Pb(btsa)$_2$, 0.5 s $SnCl_4$ pulse and 5.0 s purge durations. Thicknesses were measured with EDS except for (d), where the thicknesses used to calculate uniformity were measured with ellipsometry.

2.3 $(Pb(gem))_2$ and $SnCl_4$ process

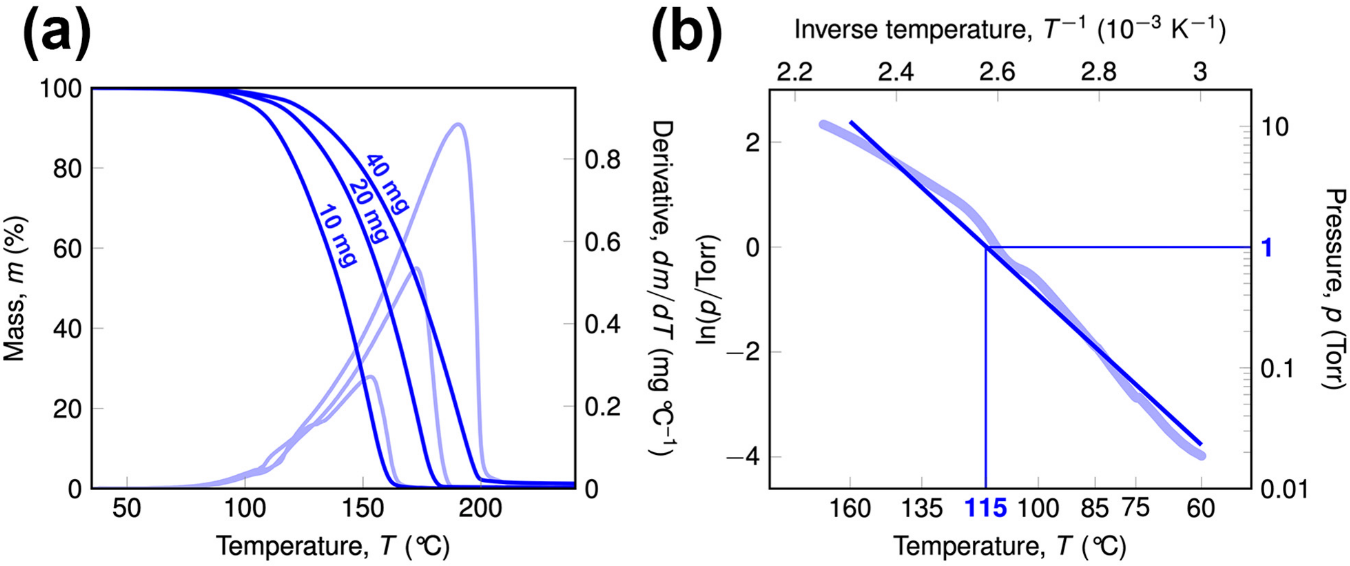

Figure S3. (a) Thermogravimetric analysis (TGA) of $(Pb(gem))_2$ under a flow of N_2 at a ramp rate of 10 °C/min with approximate initial mass loadings of 10, 20, and 40 mg (dark blue) and the respective derivative of mass with respect to temperature (light blue). (b) Vapour pressure of $(Pb(gem))_2$ estimated using TGA data from (d, light blue) and a linear trend between the inverse temperature and natural logarithm of the vapour pressure (dark blue) with an approximately 20 mg initial mass loading. The precursor achieves a vapour pressure of 1 Torr at 115 °C.

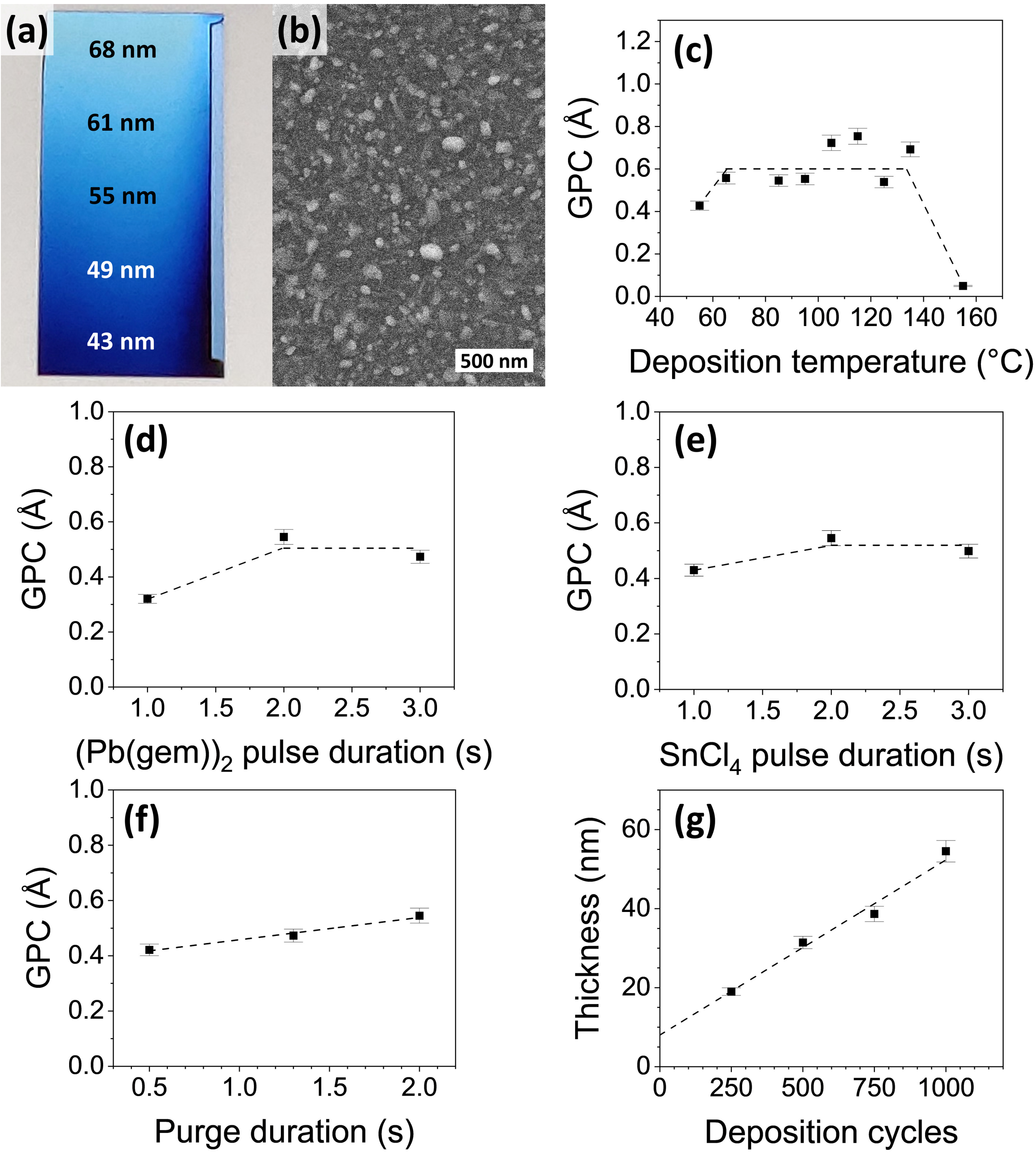

(h)

Composition (ToF-ERDA)	
Element	**Concentration (at%)**
Cl	29.0 ± 1.0
Pb	14.5 ± 1.0
Sn	15.9 ± 1.0
O	23.0 ± 1.0
N	1.2 ± 0.5
C	4.2 ± 1.0
H	12.5 ± 1.0

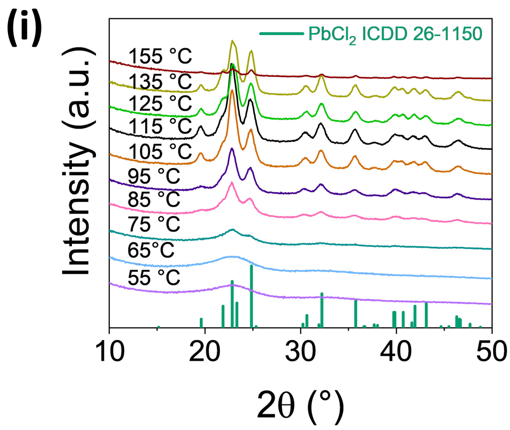

Figure S4. (a) Digital photograph and (b) FESEM image of a $PbCl_2$ film. In (a) film thickness measured by ellipsometry is shown across the 5 cm long Si substrate. GPC of $PbCl_2$ as a function of (c) deposition temperature, (d) $(Pb(gem))_2$ pulse, (e) $SnCl_4$ pulse and (f) purge duration. (g) Thickness as a function deposition cycles. (h) ToF-ERDA composition of a $PbCl_2$ film. (i) XRD patterns of the $PbCl_2$ films deposited at different temperatures. Unless otherwise evident, the data in this figure is from depositions made at 85 °C with 1000 cycles, 2.0 s $(Pb(gem))_2$, 2.0 s $SnCl_4$ pulse and 2.0 s purge durations. Thicknesses were measured with EDS unless stated otherwise.

2.4 $Pb(btsa)_2$ and $GaCl_3$ process

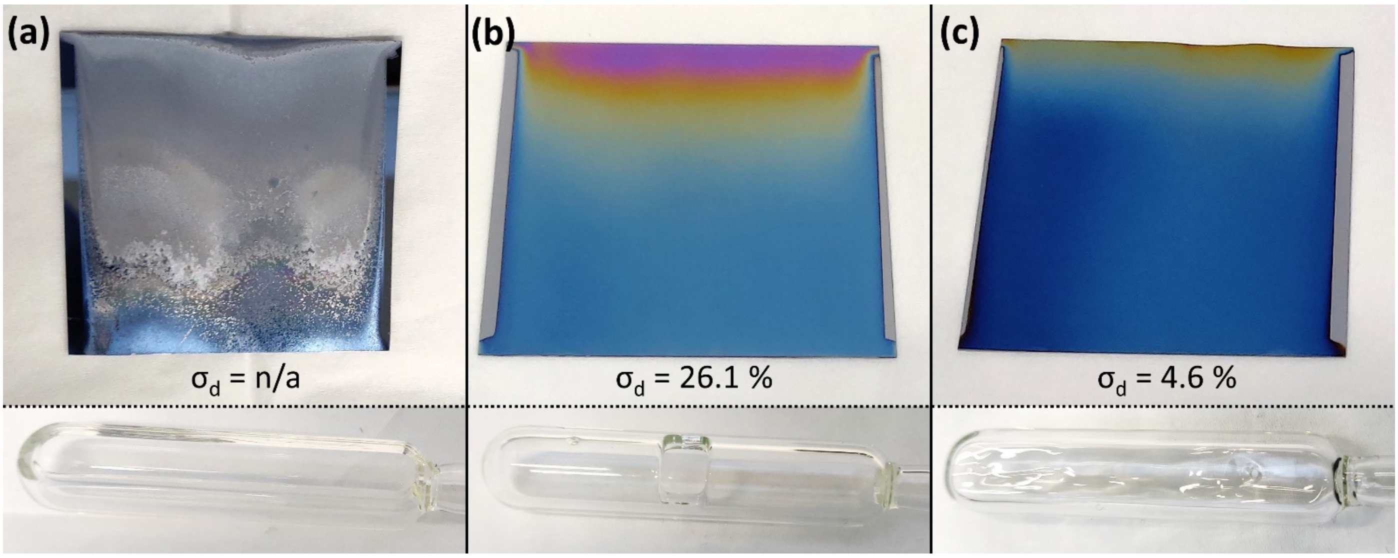

Figure S5. Digital photographs of PbCl2 films (top) deposited with $GaCl_3$ sublimed from different containers (bottom). In (a) open glass boat was used, and the film was deposited at 75 °C with 1000 cycles. The pulse durations were 1.0 s and 0.5 s for $Pb(btsa)_2$ and $GaCl_3$ respectively. The purge duration between precursor pulses was 2.0 s. In (b) a closed glass boat with a 7x5mm orifice was used and the film was deposited at 85 °C with 600 cycles. The pulse durations were 1.5 s and 0.4 s for $Pb(btsa)_2$ and $GaCl_3$ respectively. The purge duration between precursor pulses was 3.0 s. In (c) a closed glass boat with a 1 mm ø orifice and the film was deposited at 85 °C with 600 cycles. The pulse durations were 1.5 s and 0.8 s for $Pb(btsa)_2$ and $GaCl_3$ respectively. The purge duration between precursor pulses was 3.0 s. Thickness nonuniformity (σ_d) is expressed as standard deviation of thicknesses measured from 81 points. The points were distributed 0.5 cm from each other in a 9x9 grid across the substrate. The thickness was measured with ellipsometry. This approach did not work for the film in (a) due to the poor quality of the film. Ellipsometry thickness maps of the films in (b) and (c) are shown in Figure S6.

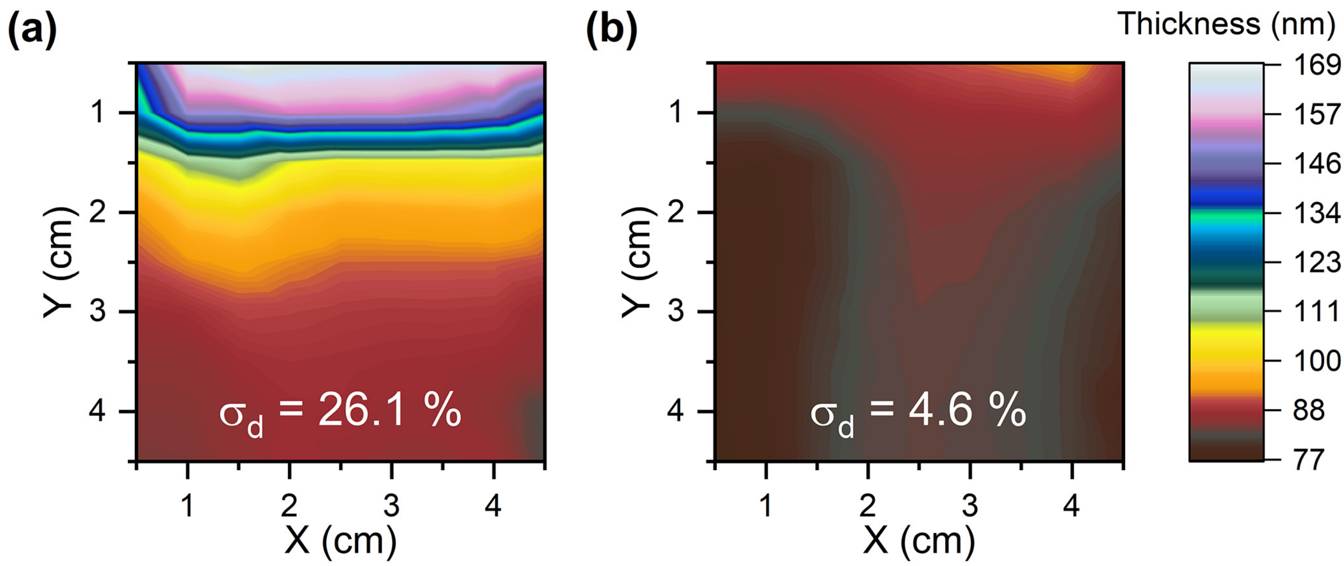

Figure S6. Ellipsometry thickness maps of $PbCl_2$ films deposited on 5 x 5 cm Si substrates (0.5 cm edge exclusion). Precursor flow direction is top-down. In (a) and (b) $GaCl_3$ was sublimed from closed glass boats with 7x5 mm and 1 mm orifices respectively. The films were deposited at 85 °C with 600 cycles. $Pb(btsa)_2$ pulse duration was 1.5 s and $GaCl_3$ pulse duration was 0.4 s in (a) and 0.8 s in (b). Purge duration between the precursor pulses was 3.0 s. For more details see Figure S5.

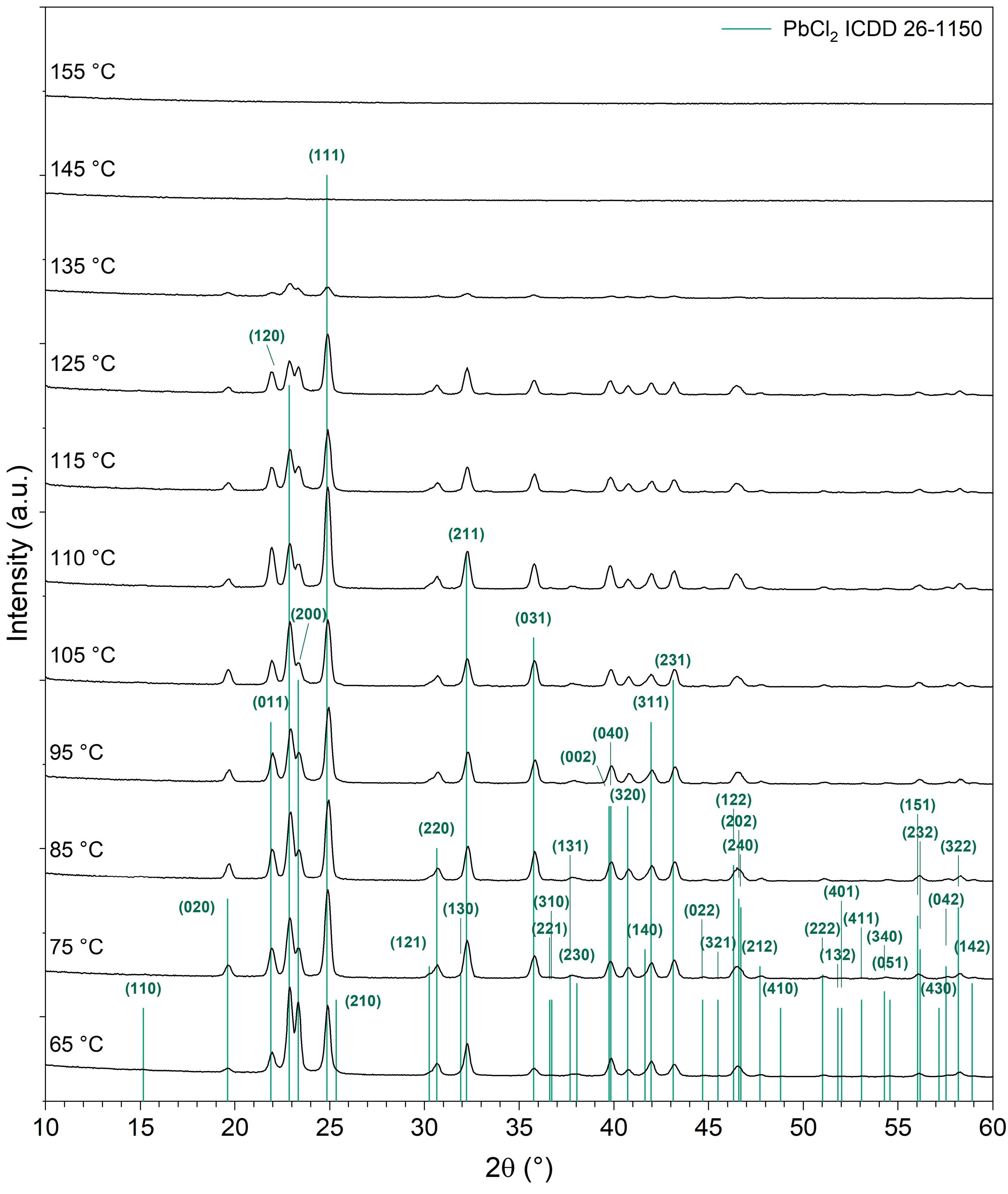

Figure S7. XRD patterns of $PbCl_2$ films deposited with $Pb(btsa)_2$ and $GaCl_3$ at different temperatures. The films were deposited with 600 cycles of 1.5 s $Pb(btsa)_2$ pulse, 0.8 s $GaCl_3$ pulse and 3.0 s purge durations.

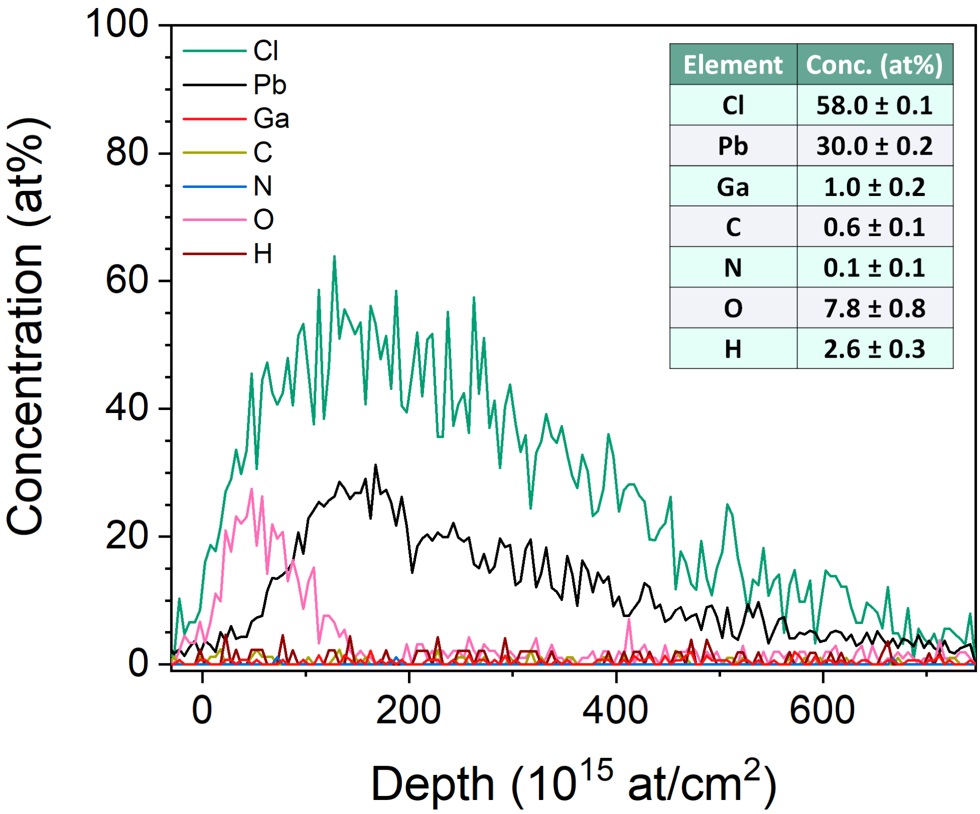

Element	Conc. (at%)
Cl	58.0 ± 0.1
Pb	30.0 ± 0.2
Ga	1.0 ± 0.2
C	0.6 ± 0.1
N	0.1 ± 0.1
O	7.8 ± 0.8
H	2.6 ± 0.3

Figure S8. Elemental depth profile and composition of a $PbCl_2$ film as analysed by ToF-ERDA. The $PbCl_2$ film was deposited at 85 °C with 600 cycles of 1.5 s and 0.8 s long pulses of $Pb(btsa)_2$ and $GaCl_3$ respectively, separated by 3.0 s long purges.

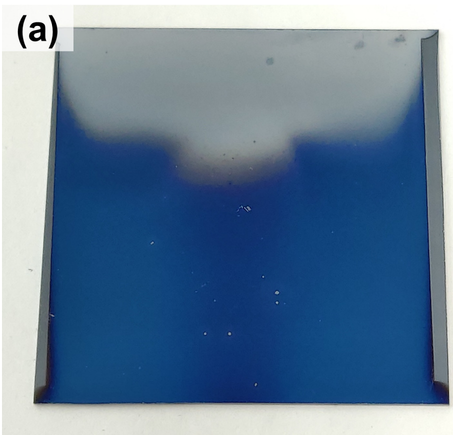

(b)

Element	EDS Concentration (at%)	
	2 h	15 days
Cl	68.0	64.7
Pb	27.1	25.9
O	4.9	9.4

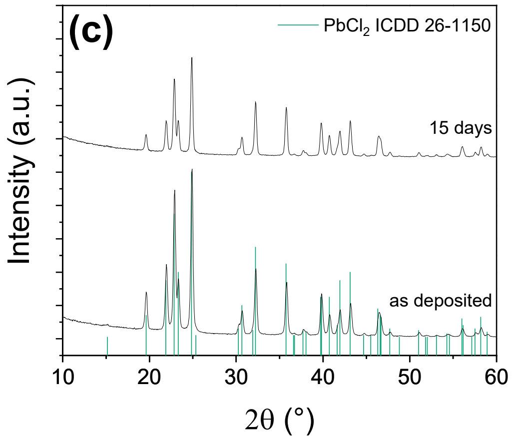

Figure S9. (a) Digital photograph of a $PbCl_2$ film stored in air for 15 days. (b) EDS concentration of Pb, Cl and O in a $PbCl_2$ film after the deposition and after storage in air for 15 days. An ultrathin window in our EDS detector allows to measure X-rays produced by lighter elements ($Z < 11$) such as oxygen but the accuracy of their concentration values can be low (commonly overestimated). Nevertheless, the observed trends are reliable: the oxygen k-ratio increased from 0.00059 (2 h) to 0.00107 (15 days). (c) XRD pattern of a $PbCl_2$ film as deposited and after storage in air for 15 days. The $PbCl_2$ film was deposited at 85 °C with 600 cycles of 1.5 s and 0.8 s long pulses of $Pb(btsa)_2$ and $GaCl_3$ respectively, separated by 3.0 s long purges.

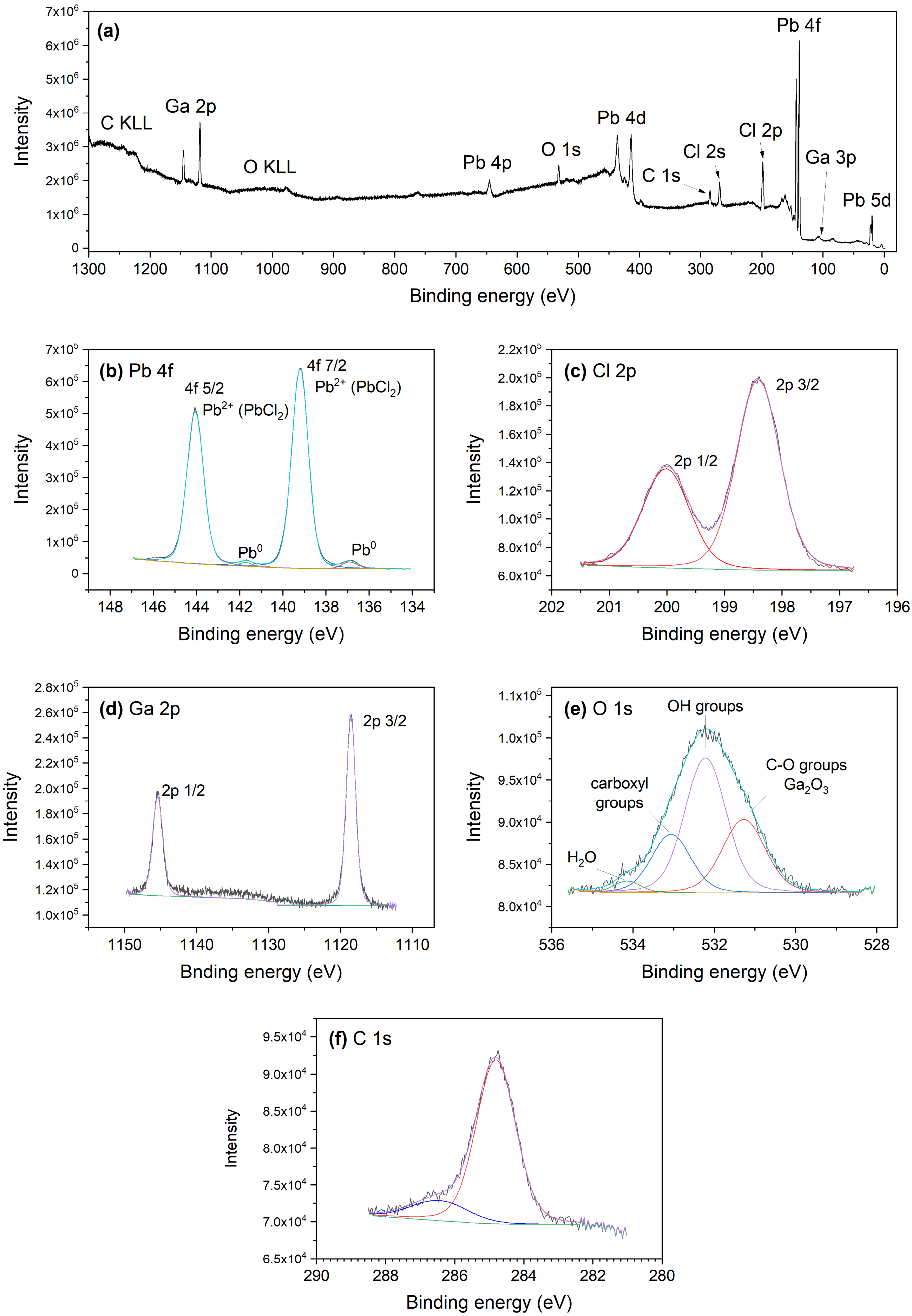

Figure S10. (a) XPS spectra of a $PbCl_2$ film as well as high resolution spectra of Pb 4f (b), Cl 2p (c), Ga 2p (d), O 1s (e) and C 1s (f). The $PbCl_2$ film was deposited at 85 °C with 600 cycles of 1.5 s and 0.8 s long pulses of $Pb(btsa)_2$ and $GaCl_3$ respectively, separated by 3.0 s long purges.

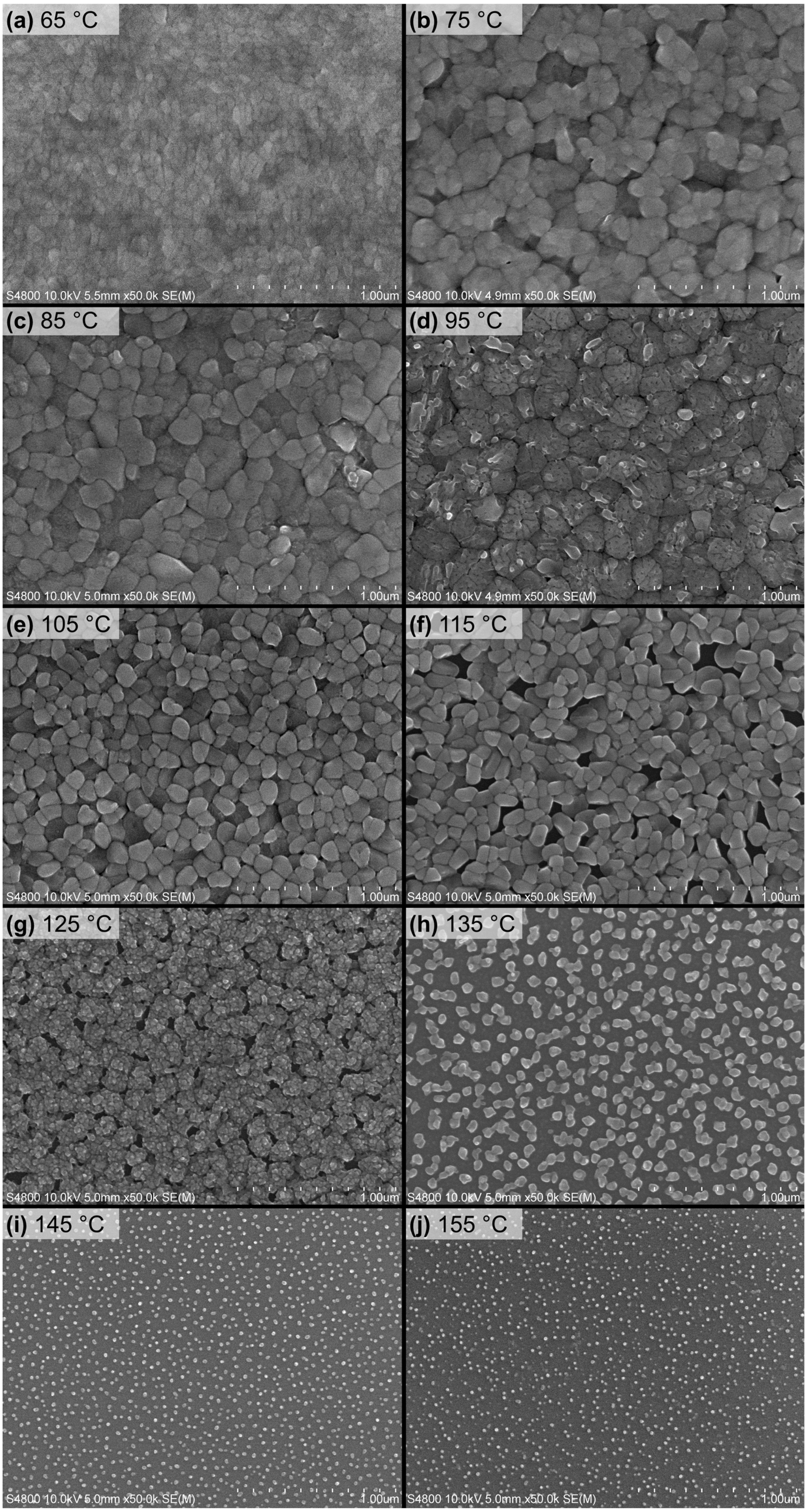

Figure S11. Top down FESEM images of $PbCl_2$ films deposited at different temperatures. The films were deposited with 600 cycles of 1.5 s $Pb(btsa)_2$ pulse, 0.8 s $GaCl_3$ pulse and 3.0 s purge durations.

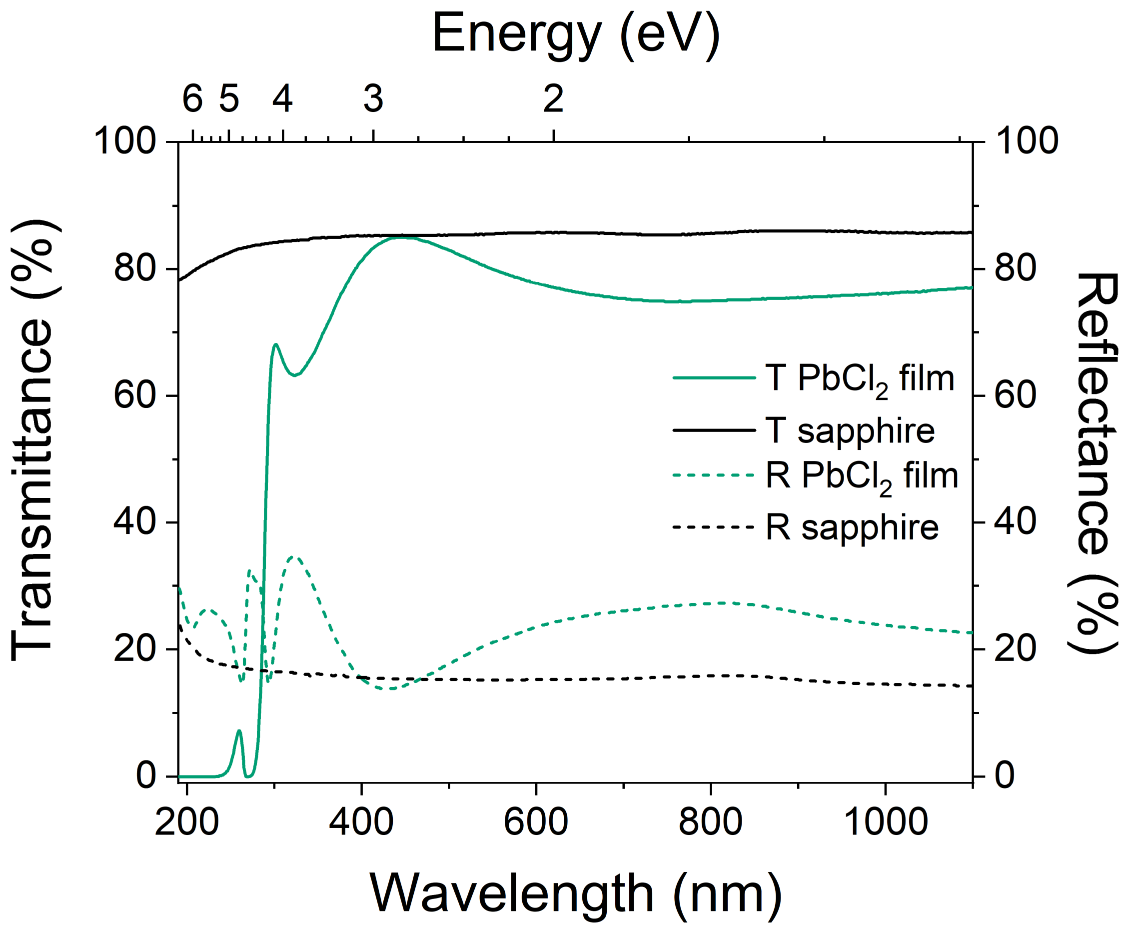

Figure S12. Transmittance and reflectance of a $PbCl_2$ film deposited at 85 °C, with 600 cycles of 1.5 s $Pb(btsa)_2$, 0.8 s $GaCl_3$ pulse and 3.0 s purge durations. An evaporated aluminium mirror served as a reference for reflectance measurements.

2.5 $Pb(btsa)_2$ and $SnBr_4$ process

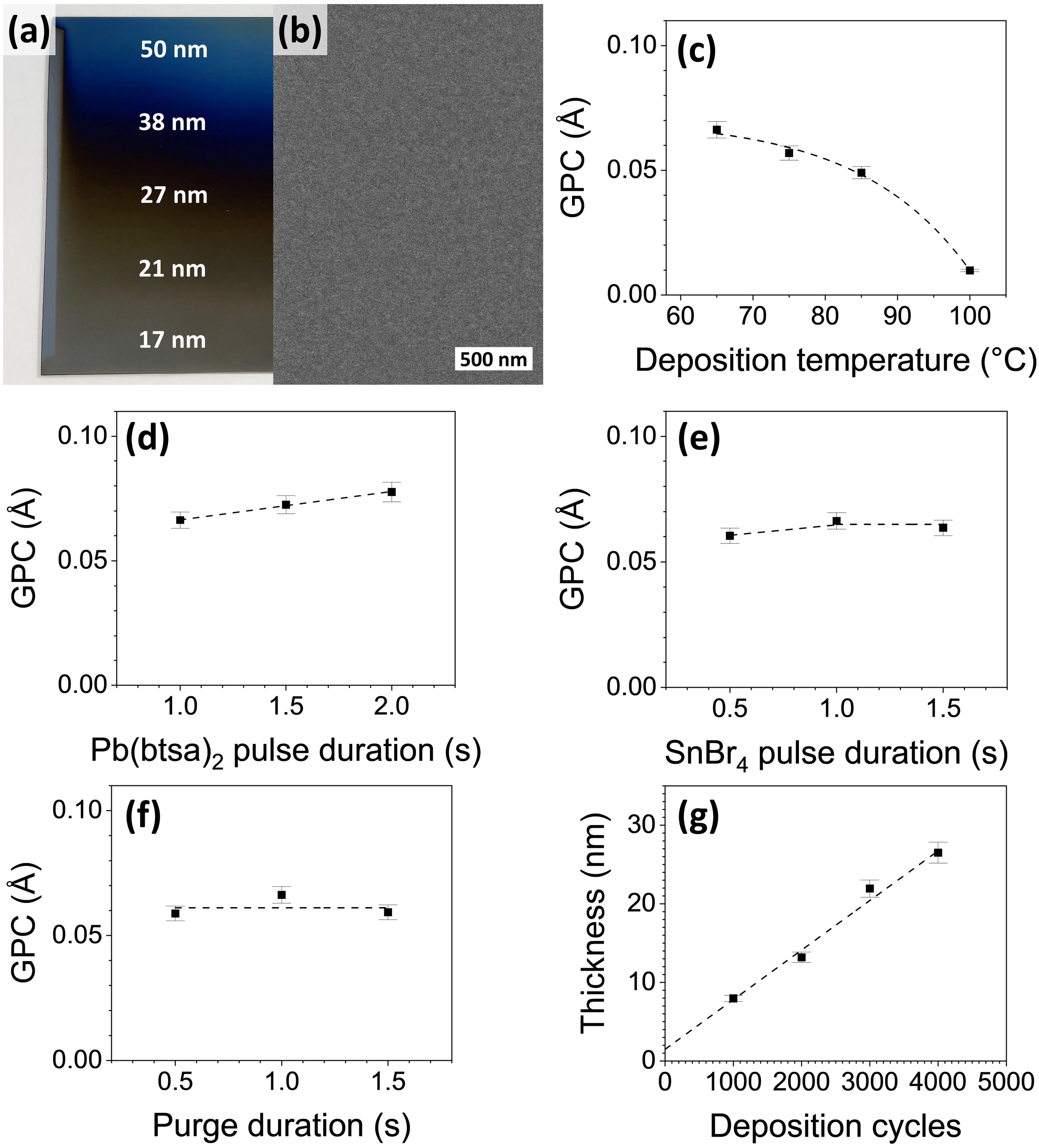

(h) Composition (ToF-ERDA)

Element	Concentration (at%)
Br	33. 4 ± 1.0
Pb	17.7 ± 1.0
Sn	7.8 ± 1.0
O	20.3 ± 1.0
N	1.1 ± 0.5
C	2.8 ± 0.5
H	16.9 ± 1.0

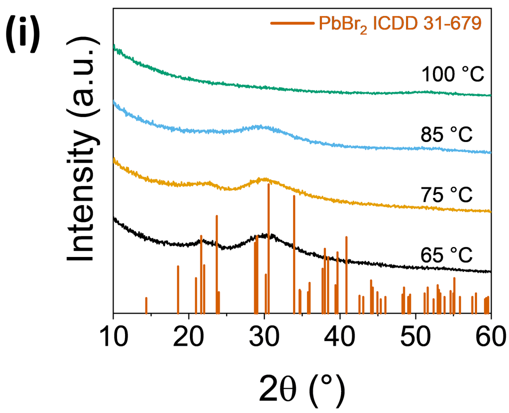

Figure S13. (a) Digital photograph and (b) FESEM image of a $PbBr_2$ film. In (a) film thickness measured by ellipsometry is shown across the 5 cm long Si substrate. GPC of $PbBr_2$ as a function of (c) deposition temperature, (d) $Pb(btsa)_2$ pulse, (e) $SnBr_4$ pulse, and (f) purge duration. (g) Thickness as a function deposition cycles. (h) ToF-ERDA composition of a $PbBr_2$ film. (i) XRD patterns of $PbBr_2$ films deposited at different temperatures. Unless otherwise evident, the data in this figure is from depositions made at 65 °C with 4000 cycles, 1.0 s $Pb(btsa)_2$, 1.0 s $SnBr_4$ pulse and 1.0 s purge durations. Thicknesses were measured with EDS unless stated otherwise.

2.6 Pb(btsa)$_2$ and TiBr$_4$ process

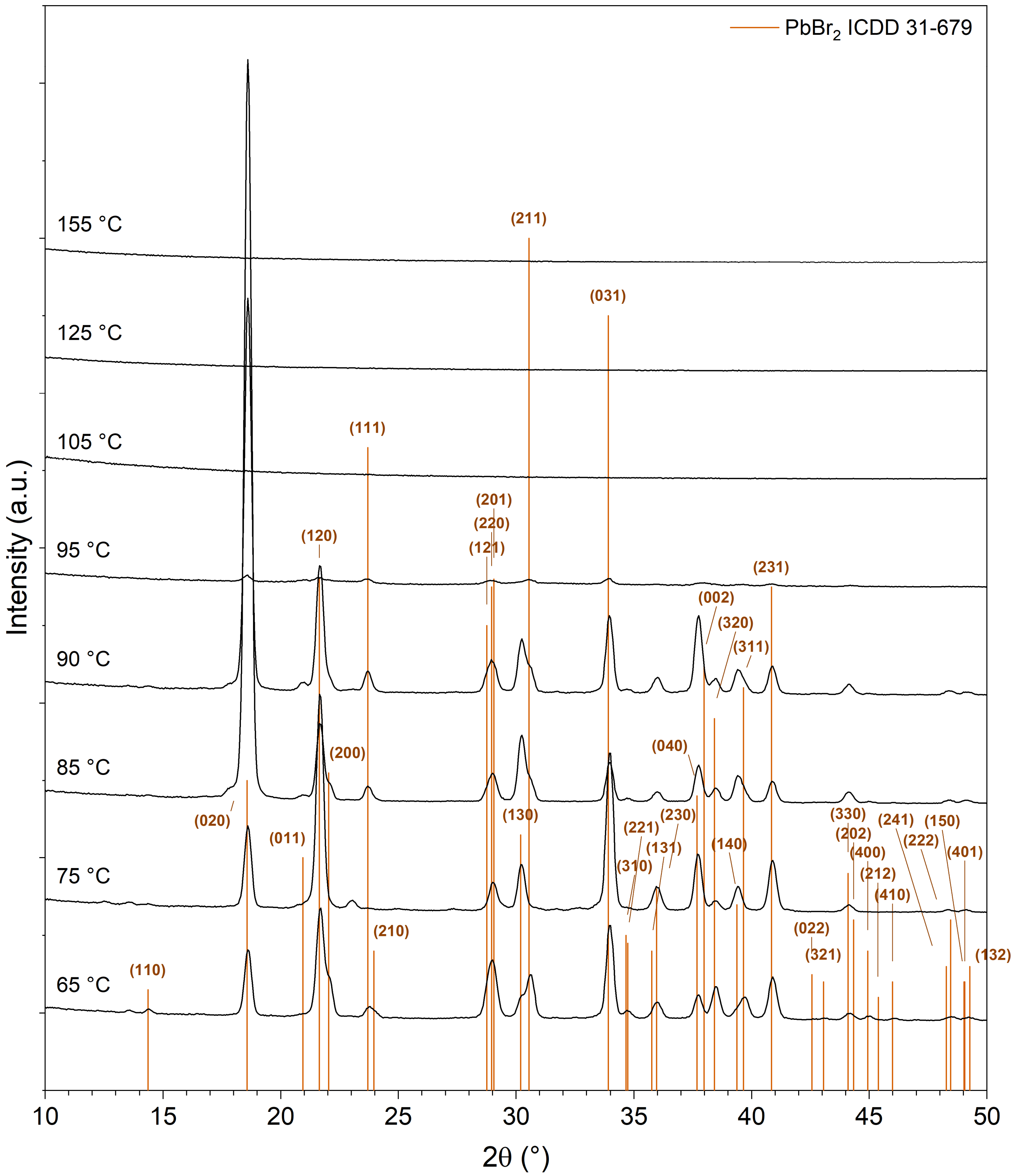

Figure S14. XRD patterns of PbBr$_2$ films deposited with Pb(btsa)$_2$ and TiBr$_4$ at different temperatures. The films were deposited with 1000 cycles. The pulse durations were 1.0 s and 1.5 s long for Pb(btsa)$_2$ and TiBr$_4$ respectively and were separated by 1.0 s long purges.

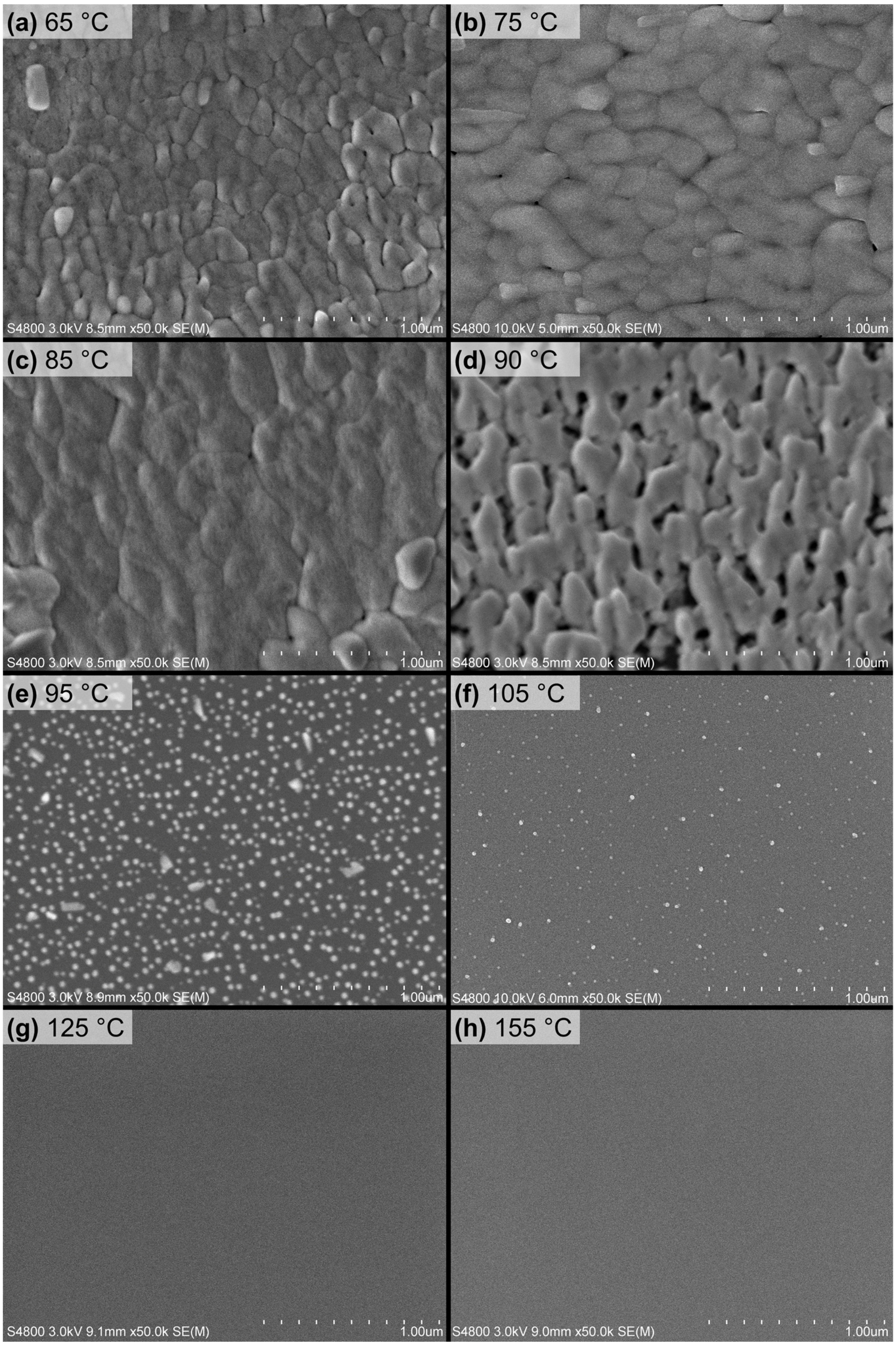

Figure S15. Top down FESEM images of $PbBr_2$ films deposited at different temperatures. The films were deposited with 1000 cycles of 1.0 s $Pb(btsa)_2$ pulse, 1.5 s $TiBr_4$ pulse and 1.0 s purge durations.

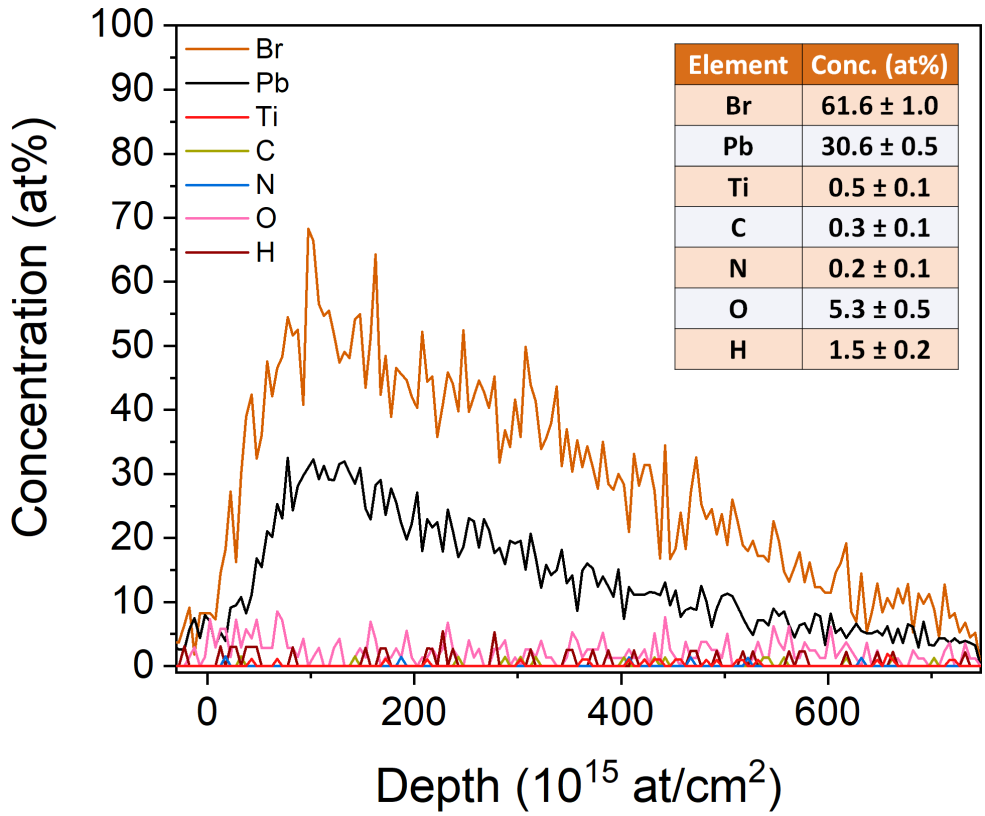

Figure S16. Elemental depth profile and composition of a $PbBr_2$ film as analysed by ToF-ERDA. The $PbBr_2$ film was deposited at 75 °C with 1000 cycles of 1.0 s $Pb(btsa)_2$ pulse, 1.5 s $TiBr_4$ pulse and 1.0 s purge durations.

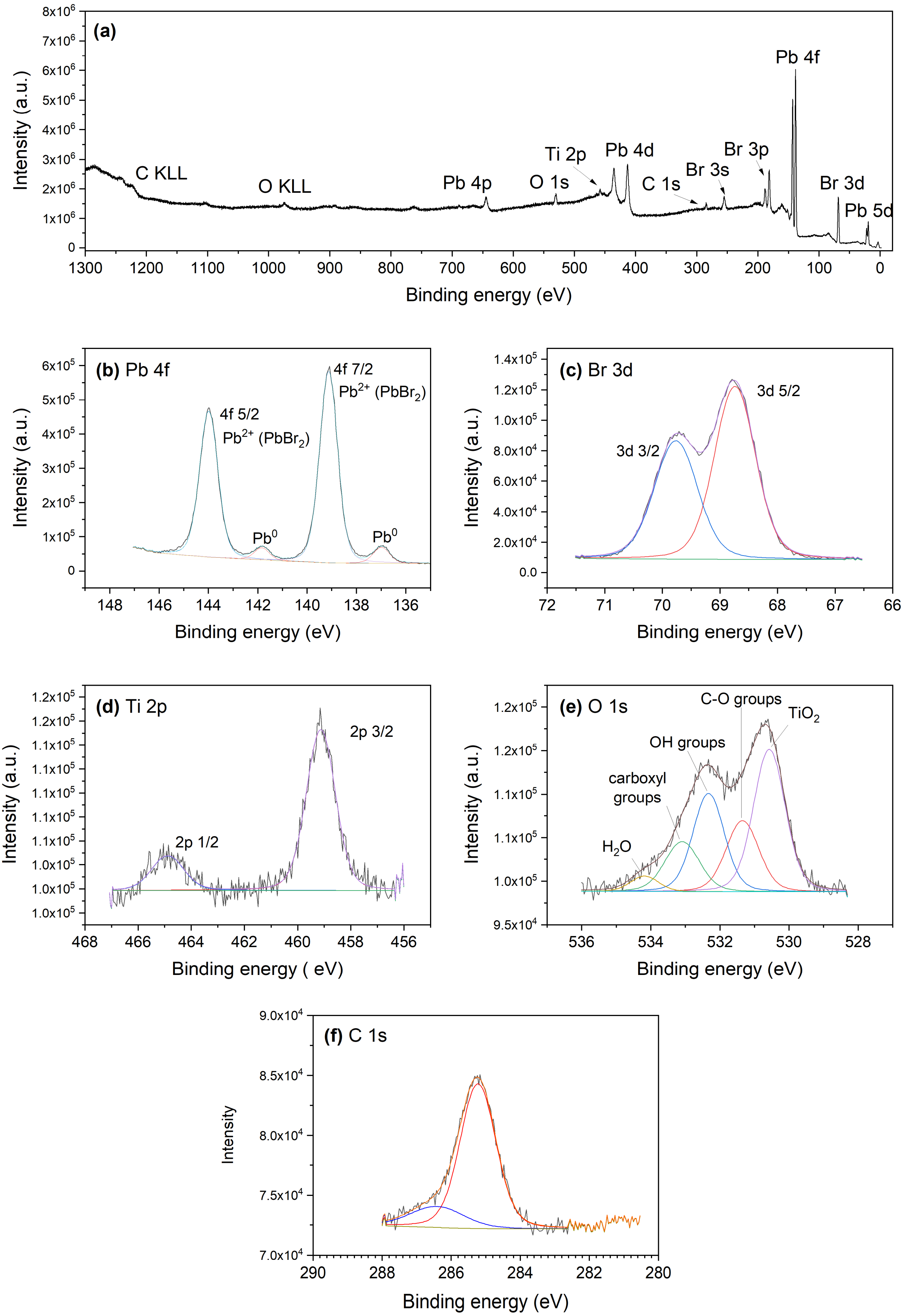

Figure S17. (a) XPS spectra of a $PbBr_2$ film as well as high resolution spectra of Pb 4f (b), Cl 2p (c), Ti 2p (d), O 1s (e) and C 1s (f). The $PbBr_2$ film was deposited at 75 °C with 1000 cycles of 1.0 s $Pb(btsa)_2$ pulse, 1.5 s $TiBr_4$ pulse and 1.0 s purge durations.

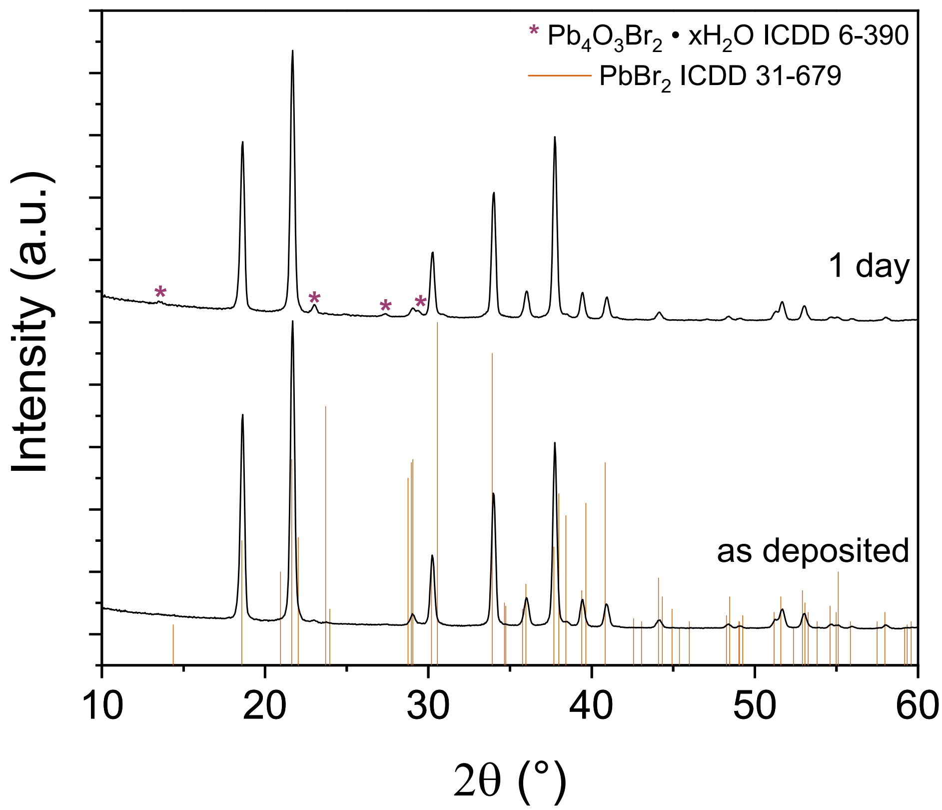

Figure S18. XRD pattern of a $PbBr_2$ film as deposited and after storage in ambient air for 1 day. The film was deposited at 75 °C with 1000 cycles of 1.0 s $Pb(btsa)_2$ pulse, 1.5 s $TiBr_4$ pulse and 1.0 s purge durations. The as deposited sample is still exposed to air during the transfer between the ALD reactor and diffractometer.

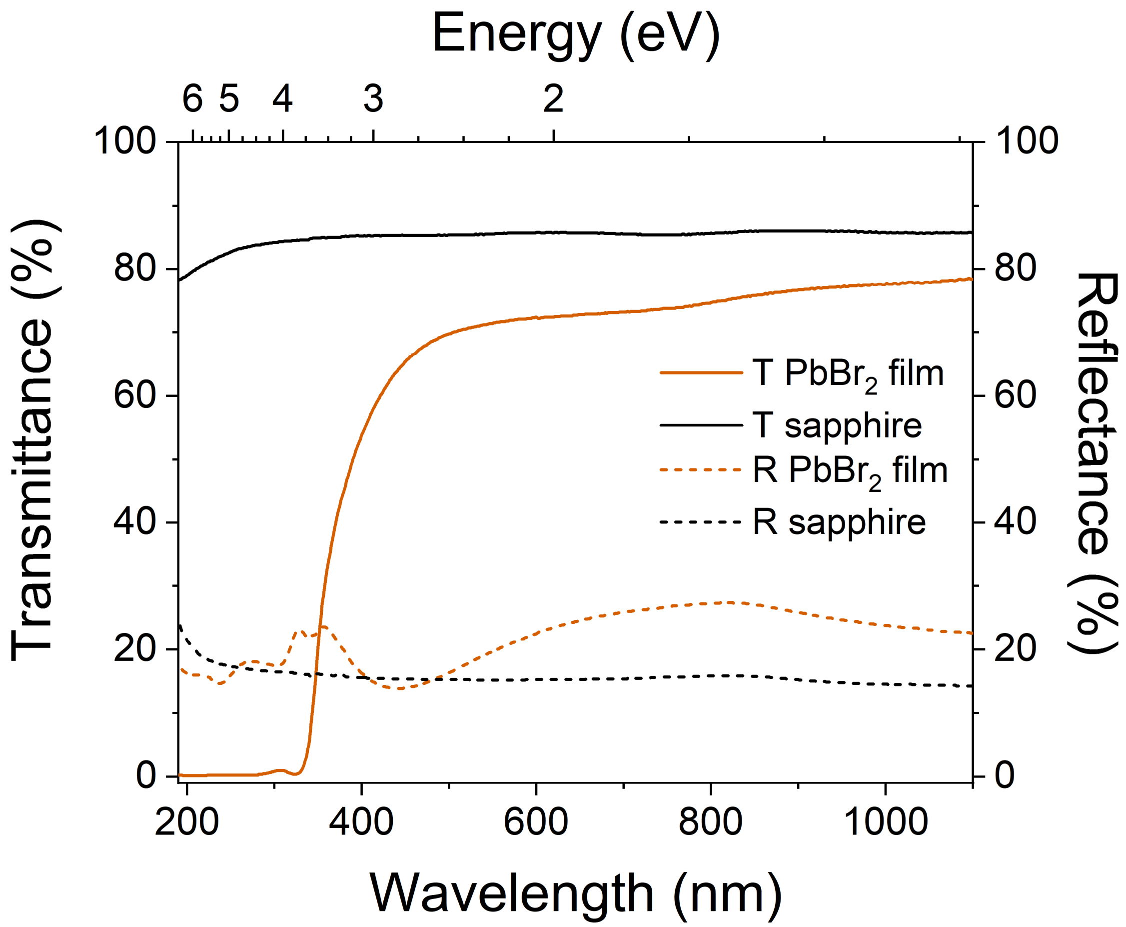

Figure S19. Transmittance and reflectance of a $PbBr_2$ film deposited at 75 °C, with 1000 cycles of 1.0 s $Pb(btsa)_2$, 1.5 s $TiBr_4$ pulse and 1.0 s purge durations. An evaporated aluminium mirror served as a reference for reflectance measurements.

2.7 Mixed lead halides

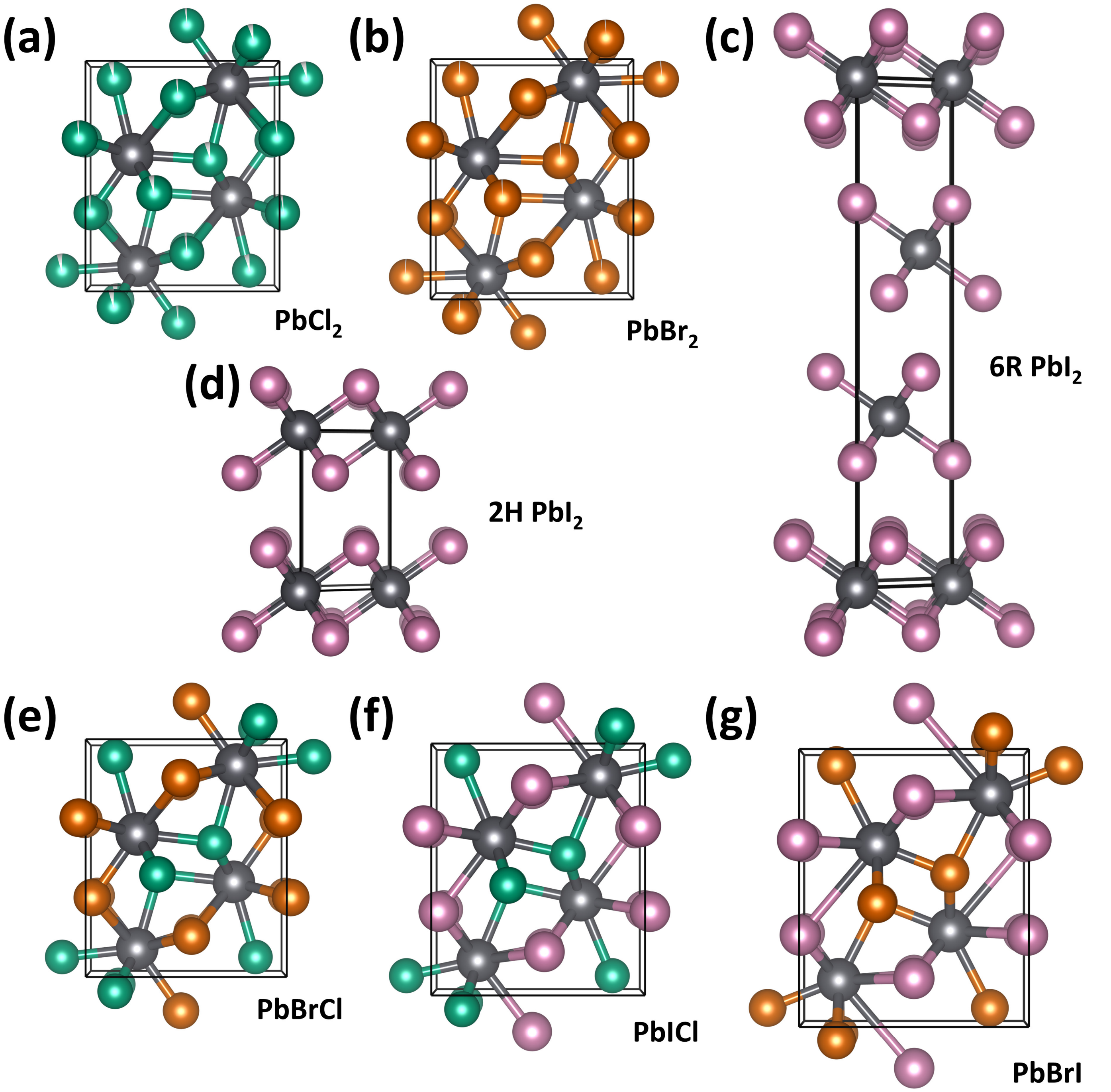

Figure S20. Unit cells of (a) $PbCl_2$ (ICSD 202130), (b) $PbBr_2$ (ICSD 202134), (c) 6R PbI_2 (ICSD 24265), (d) 2H PbI_2 (ICSD 68819), (e) PbBrCl (ICSD 22136), (f) PbICl (ICSD 22137) and (g) PbBrI (ICSD 22138). For PbI_2 polytype structures the view is along *a* and for cotunnite structures along *c*. Figure made with VESTA (see Momma et al. *J. Appl. Crystallogr.* **2011**, 44, 1272–1276, doi: 10.1107/S0021889811038970).

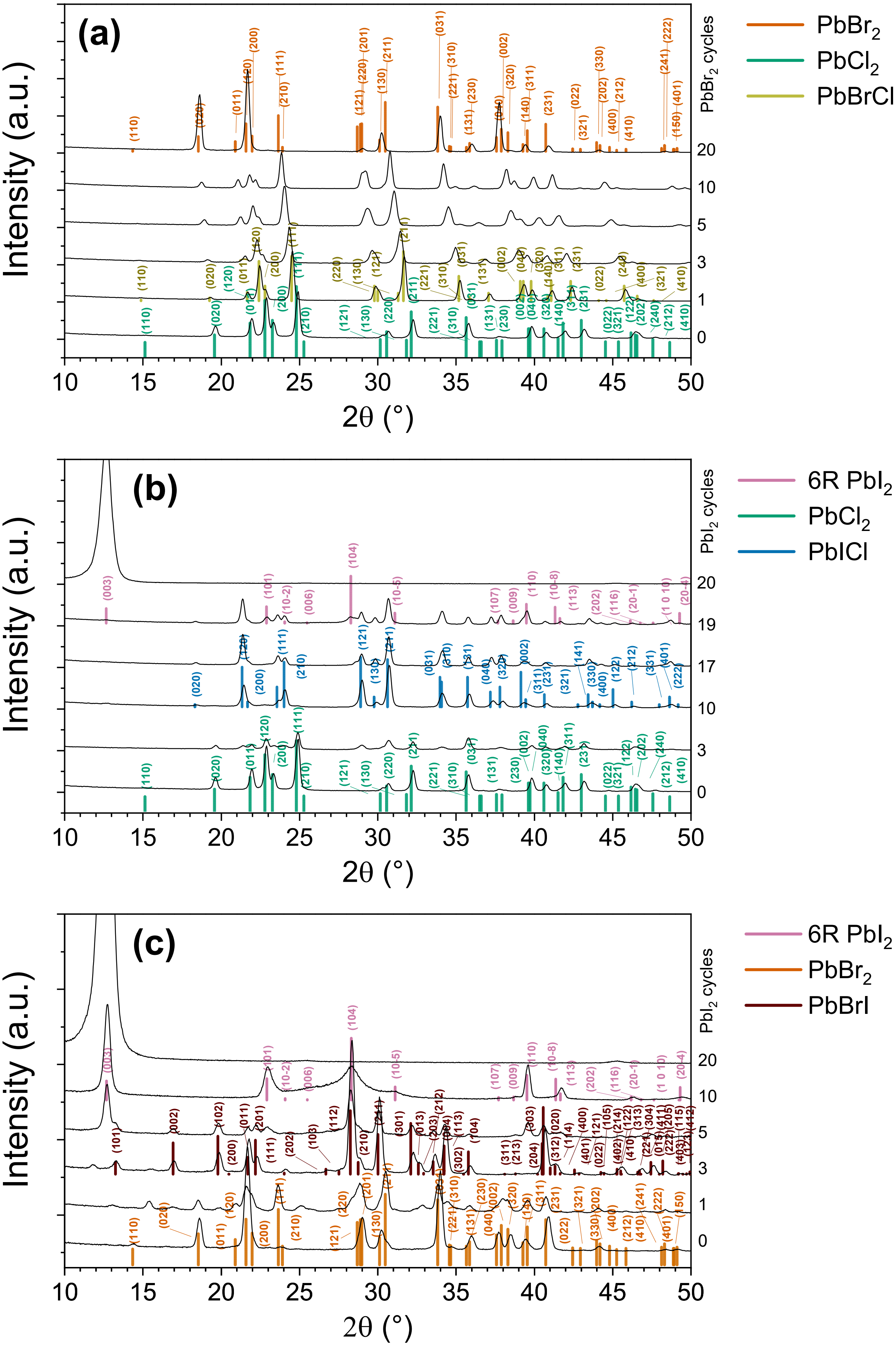

Figure S21. XRD patterns of (a) $PbBr_xCl_{2-x}$, (b) PbI_xCl_{2-x} and $PbBr_xI_{2-x}$ films. Relevant XRD reference patterns, including $PbBr_2$ (ICDD 31-679), $PbCl_2$ (ICDD 26-1150), PbBrCl (ICDD 24-1088), 6R PbI_2 (COD 9009142), PbICl (ICDD 43-949) and PbBrI (ICSD 22138) are shown. All films were deposited at 75 °C.

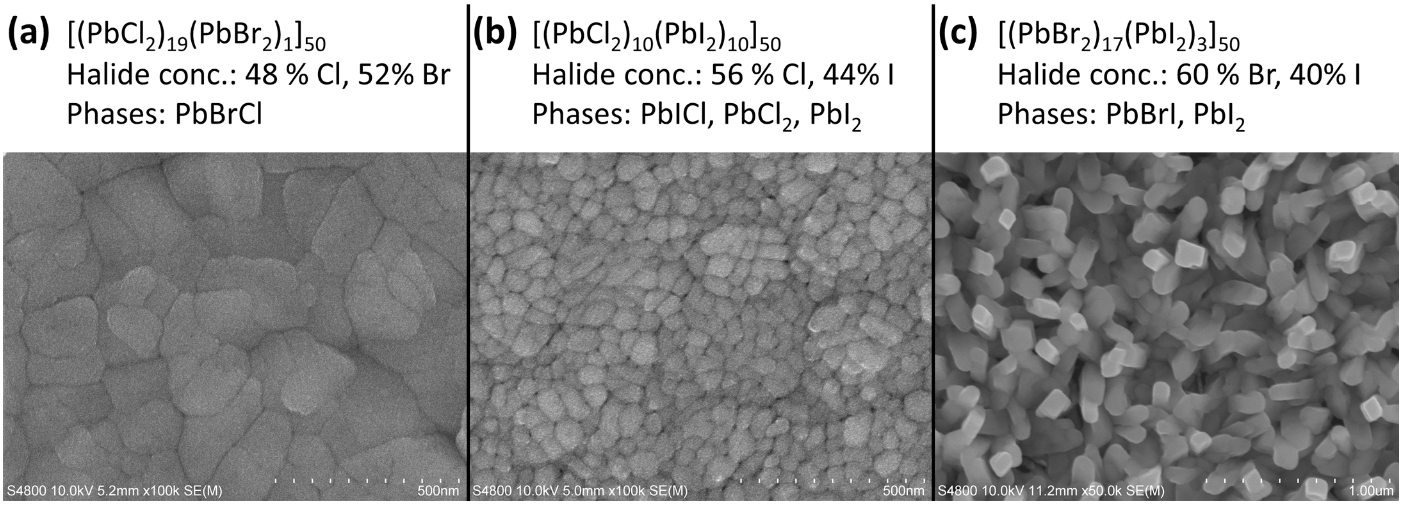

Figure S22. FESEM images of selected mixed lead halide films deposited at 75 °C.

4.5 Quantum chemical calculations

Table S1. Electronic energy plus free energy correction (E(el) + G), free energy correction (G), enthalpy correction (H), and entropy correction at STP (S*298.15) in Hartrees for relevant metal chloride species.

NAME	E(el) + G	G	H	S*298.15
Pb(btsa)Cl	-1526.262595	0.18129847	0.24804604	0.06769177
Pb(btsa)Cl_3	-2446.645099	0.17972302	0.25447745	0.07569864
Pb$(btsa)_2Cl_2$	-2859.449316	0.39354064	0.49689543	0.104299
Pb$(btsa)_2$	-1939.046309	0.39409983	0.48979814	0.09664253
Pb$(btsa)_3$Cl	-3272.221731	0.61398079	0.74084983	0.12781325
$PbCl_2$	-1113.470064	-0.02943847	0.0060196	0.03640228
$PbCl_4$	-2033.834377	-0.03219524	0.01215188	0.04529133
Sn(btsa)Cl	-1547.681321	0.18270733	0.2484119	0.06664878
Sn(btsa)Cl_3	-2468.119351	0.18194276	0.25510282	0.07410427
Sn$(btsa)_2Cl_2$	-2880.923576	0.39609102	0.49775854	0.10261173
Sn$(btsa)_2$	-1960.468803	0.39588789	0.49038107	0.0954374
Sn$(btsa)_3$Cl	-3293.698081	0.61859766	0.74229976	0.1246463
$SnCl_2$	-1134.883649	-0.02834919	0.00609657	0.03538998
$SnCl_4$	-2055.309895	-0.0304249	0.01244175	0.04381086
Ti(btsa)Cl_3	-3103.292843	0.18409282	0.25581909	0.07267047
Ti$(btsa)_2Cl_2$	-3516.093571	0.39859722	0.49850639	0.10085337
Ti$(btsa)_3$Cl	-3928.866046	0.62240789	0.74332272	0.12185904
$TiCl_4$	-2690.480296	-0.02833658	0.01298555	0.04226633

Table S2. Electronic energy plus free energy correction (E(el) + G), free energy correction (G), enthalpy correction (H), and entropy correction at STP (S*298.15) in Hartrees for relevant metal bromide species.

NAME	E(el) + G	G	H	S*298.15
$PbBr_2$	-5341.399861	-0.03195106	0.00582758	0.03872284
$PbBr_4$	-10489.70453	-0.03657638	0.01169605	0.04921664
Pb(btsa)Br	-3640.227772	0.17908549	0.24759042	0.06944914
Pb(btsa)Br_3	-8788.544117	0.17680416	0.25411616	0.07825621
$Pb(btsa)_2Br_2$	-7087.380121	0.39164515	0.49662483	0.10592389
$Pb(btsa)_2$	-1939.046309	0.39409983	0.48979814	0.09664253
$Pb(btsa)_3Br$	-5386.184352	0.61330685	0.74079989	0.12843724
$SnBr_2$	-5362.810438	-0.03095859	0.00587778	0.03778058
$SnBr_4$	-10511.16697	-0.03508104	0.01186049	0.04788574
Sn(btsa)Br	-3661.644302	0.18134852	0.24821184	0.06780753
Sn(btsa)Br_3	-8810.009412	0.17878051	0.2546452	0.0768089
$Sn(btsa)_2Br_2$	-7108.84904	0.39398081	0.49742691	0.10439032
$Sn(btsa)_2$	-1960.468803	0.39588789	0.49038107	0.0954374
$Sn(btsa)_3Br$	-5407.657546	0.61781069	0.74224601	0.12537954
$TiBr_4$	-11146.31541	-0.03316416	0.01228227	0.04639064
Ti(btsa)Br_3	-9445.167375	0.18079771	0.25527394	0.07542044
$Ti(btsa)_2Br_2$	-7744.009705	0.3966616	0.49817213	0.10245475
$Ti(btsa)_3Br$	-6042.821149	0.62161971	0.7432596	0.12258411

Table S3. Electronic energy plus free energy correction (E(el) + G), free energy correction (G), enthalpy correction (H), and entropy correction at STP (S*298.15) in Hartrees for relevant metal iodide species.

NAME	E(el) + G	G	H	S*298.15
Pb(btsa)I	-1363.827256	0.17818286	0.24737449	0.07013584
Pb(btsa)I_3	-1959.349883	0.17470748	0.25393364	0.08017037
Pb$(btsa)_2I_2$	-2534.580961	0.3901587	0.49638749	0.107173
Pb$(btsa)_2$	-1939.046309	0.39409983	0.48979814	0.09664253
Pb$(btsa)_3$I	-3109.781048	0.61297204	0.74083023	0.1288024
PbI_2	-788.6000028	-0.0336154	0.00576245	0.04032206
PbI_4	-1384.118949	-0.03944847	0.01153914	0.05193182
Sn(btsa)I	-1385.242744	0.17908509	0.24768704	0.06954616
Sn(btsa)I_3	-1980.804316	0.17669345	0.25441459	0.07866535
Sn$(btsa)_2I_2$	-2556.043219	0.39234676	0.49717862	0.10577607
Sn$(btsa)_2$	-1960.468803	0.39588789	0.49038107	0.0954374
Sn$(btsa)_3$I	-3131.249833	0.61758897	0.74230082	0.12565605
SnI_2	-810.0073087	-0.03266975	0.00579765	0.0394116
SnI_4	-1405.566241	-0.03812319	0.0116401	0.0507075
Ti(btsa)I_3	-2615.941638	0.18409282	0.25581909	0.07267047
Ti$(btsa)_2I_2$	-3191.19143	0.39539581	0.49795228	0.10350068
Ti$(btsa)_3$I	-3766.407676	0.62138826	0.74333345	0.1228894
TiI_4	-2040.685312	-0.03624123	0.01195604	0.04914148